View metadata, citation and similar papers at core.ac.uk
brought to you by CORE
provided by Online Research Database In Technology

Technical University of Denmark

Low pressure water vapour plasma treatment of surfaces for biomolecules decontamination.

Fumagalli, F; Kylian, O; Amato, Letizia; Hanus, J; Rossi, F

Published in:
Journal of Physics D: Applied Physics

Link to article, DOI:
10.1088/0022-3727/45/13/135203

Publication date:
2012

Document Version
Publisher's PDF, also known as Version of record

Link back to DTU Orbit

Citation (APA):
Fumagalli, F., Kylian, O., Amato, L., Hanus, J., & Rossi, F. (2012). Low pressure water vapour plasma treatment of surfaces for biomolecules decontamination. Journal of Physics D: Applied Physics, 45(13), 135203. DOI: 10.1088/0022-3727/45/13/135203

DTU Library
Technical Information Center of Denmark

General rights
Copyright and moral rights for the publications made accessible in the public portal are retained by the authors and/or other copyright owners and it is a condition of accessing publications that users recognise and abide by the legal requirements associated with these rights.

- Users may download and print one copy of any publication from the public portal for the purpose of private study or research.
- You may not further distribute the material or use it for any profit-making activity or commercial gain
- You may freely distribute the URL identifying the publication in the public portal

If you believe that this document breaches copyright please contact us providing details, and we will remove access to the work immediately and investigate your claim.

IOPscience iopscience.iop.org

Home Search Collections Journals About Contact us My IOPscience

Low-pressure water vapour plasma treatment of surfaces for biomolecules decontamination

This article has been downloaded from IOPscience. Please scroll down to see the full text article.

2012 J. Phys. D: Appl. Phys. 45 135203

(http://iopscience.iop.org/0022-3727/45/13/135203)

View the table of contents for this issue, or go to the journal homepage for more

Download details:
IP Address: 192.38.67.112
The article was downloaded on 17/03/2012 at 08:18

Please note that terms and conditions apply.

J. Phys. D: Appl. Phys. **45** (2012) 135203 (9pp) doi:10.1088/0022-3727/45/13/135203

Low-pressure water vapour plasma treatment of surfaces for biomolecules decontamination

F Fumagalli[1], O Kylián[2], L Amato[1,3], J Hanuš[1] and F Rossi[1]

[1] European Commission, Joint Research Centre, Institute for Health and Consumer Protection, Via E. Fermi 2749, 21027 Ispra (VA), Italy
[2] Faculty of Mathematics and Physics, Charles University, V Holešovičkách 2, Prague 8, 18000, Czech Republic
[3] Department of Micro and Nanotechnology, Technical University of Denmark, Produktionstorvet Bldg 423, Kgs. Lyngby, 2800, Denmark

E-mail: francois.rossi@jrc.ec.europa.eu

Received 2 December 2011, in final form 6 February 2012
Published 15 March 2012
Online at stacks.iop.org/JPhysD/45/135203

Abstract
Decontamination treatments of surfaces are performed on bacterial spores, albumin and brain homogenate used as models of biological contaminations in a low-pressure, inductively coupled plasma reactor operated with water-vapour-based gas mixtures. It is shown that removal of contamination can be achieved using pure H_2O or Ar/H_2O mixtures at low temperatures with removal rates comparable to oxygen-based mixtures. Particle fluxes (Ar^+ ions, O and H atomic radicals and OH molecular radicals) from water vapour discharge are measured by optical emission spectroscopy and Langmuir probe under several operating conditions. Analysis of particle fluxes and removal rates measurements illustrates the role of ion bombardment associated with O radicals, governing the removal rates of organic matter. Auxiliary role of hydroxyl radicals is discussed on the basis of experimental data. The advantages of a water vapour plasma process are discussed for practical applications in medical devices decontamination.

1. Introduction

Elimination of potentially harmful microorganisms and biomolecules present on surfaces is a major concern in many different technological areas, for instance food, packaging, textiles or aerospace industries. However, the field where sterilization and decontamination are of paramount importance is the medical praxis, where these processes represent a crucial step in guaranteeing the safety of patients. This is especially true for the cases of reused instruments, such as endoscopes, dental drills or surgical tools where remaining biological contamination is a major concern [1, 2].

However, in most of the cases mentioned above, surface sterilization and decontamination cannot be achieved with the currently available technologies. Drawbacks in actual sterilization processes are related in particular to the high resistance of certain biomolecules, for instance prions, towards routine chemical and physical cleaning processes [3] or incompatibility between the materials used in biomedical applications and the process parameters [4–6]. Infectious proteins, i.e. prions, are pathogens composed of proteins in a misfolded form responsible for transmissible spongiform encephalopathies for a variety of mammals, including humans, are in this respect of particular concern [7, 8].

Plasma discharges have attracted a lot of attention in recent years, and represent a promising alternative to conventional decontamination methods since they are able to effectively eliminate various kinds of harmful biomolecules in a wide range of conditions.

Among the different working gas mixtures tested, oxygen containing gas mixtures have been proven to lead, in general, to fastest etching rates in low-pressure systems. Depending on the reactor design, Ar/O_2 gas mixtures showed best biomaterial removal efficiency in RF discharges [9–12], when treated samples were placed in to active plasma. In addition, interesting results in terms of sterilization capability of plasmas were also reached using H_2/O_2 gas mixtures [13, 14], N_2/O_2 gas mixtures [15–17] or pure O_2 discharge plasma [18, 19].

Water vapour plasma is, however, an interesting possibility to address the decontamination problem and this

 © 2012 IOP Publishing Ltd Printed in the UK & the USA

type of discharge has already been studied for several surface modification processes, such as for instance, corrosion resistance [20], polymers activation [21–23], UV light source [24] and microorganisms sterilization [25]. The rich gas-phase chemistry generated in such low-pressure plasmas comprises reactive ions as well as O, H and OH radicals [26], which all have different chemical activities and may thus contribute to the process of inactivation or removal of biological pathogens.

Furthermore, water vapour discharges are considerably cheaper, safer and easier to handle than high-purity commercial gas mixtures of hydrogen or oxygen. On the other hand, one of the limitations arising in the applications is the strong chemical reaction occurring between such plasmas and inner metal electrodes surfaces. From the very beginning, the use of electrodeless discharges (either under vacuum or at atmospheric pressure) such as inductive coupling, microwave or dielectric barrier discharge has been preferred.

In the field of decontamination, large cleaning installations will be required to treat the load of contaminated objects produced daily from a hospital facility. The main characteristics of an effective hospital-scale reactor would be (i) the capability to treat large volumes and multiple objects in a reasonably short time, (ii) the capability to treat thermo-labile materials without damage, (iii) a superior decontamination efficacy compared with actually implemented methods and finally (iv) low installation and maintenance costs. The first two tasks can be addressed employing a large-area low-pressure plasma reactor with state-of-the-art plasma sterilization and decontamination processes. The technical issues concerned with plasma sources scale-up are outside the scope of this paper, and the discussion will focus instead on the development on alternative decontamination strategies intended to fulfil the requirements of points (iii) and (iv) stated above. At the present state of research, these last two objectives present diverging requests, the most efficient discharge mixtures containing oxygen and/or hydrogen demand the installation of expensive precision gas delivery systems and severe safety protocols due to fire and explosion hazards, while a process based on water vapour may need only a simple dry vacuum evaporator tank. Water vapour plasma might represent an interesting trade-off between low costs and efficacy as long as the decontamination efficiency of such plasmas is of the same order of magnitude the ones obtained with oxygen-based gas mixtures.

The aims of this paper are (i) to test the possibility to use plasma generated in water vapours for sterilization and decontamination purposes, (ii) to compare its efficiency with other plasmas produced under identical conditions and, (iii) to identify the principal agent contributing to the removal of biological matter exposed to water vapour plasma.

2. Experimental and diagnostics

2.1. Plasma reactor

The experimental apparatus used in this work consists of a double coil planar inductive plasma reactor designed for basic studies in plasma processing and already described in detail elsewhere [27, 28]. Specifically, we used a custom-made inductively coupled plasma reactor, fully computer controlled, that allows plasma discharges to be ignited with powers up to 600 W, the working pressure range from 1 to 30 Pa and gas flows from 1 to 50 sccm with different gas mixtures comprising argon, oxygen, hydrogen and water vapour. Water vapour is simply obtained connecting a small tank containing a few millilitres of milliQ water to the vacuum chamber through a stainless-steel pipe equipped with a MKS LiquiFlow mass flow controller in order to control the water vapour partial pressure inside the reactor. The reaction chamber (5 L volume) is evacuated by a mechanical pump backed by a turbomolecular pump (Varian milliTorr L50) down to a minimum pre-vacuum pressure of 1×10^{-3} Pa. The vacuum chamber is fed by a gas inlet system composed of MKS flow controllers.

All the biological samples were treated by exposing contaminated substrates to the active region of the ICP plasma, the sample holder was placed at a distance of 55 mm from the quartz dielectric window separating the antenna from the discharge volume. Substrates (silicon, stainless steel) temperature evolution during plasma operation was monitored by means of an IR pyrometer (Raynger MX4, Raytek) operated through an IR-pass borosilicate window. Due to pulsed plasma treatment strategy chosen in our experiments (repetition frequency 100 mHz at 20% duty cycle) substrate temperature during plasma treatment remained between a minimum 25 °C and a maximum 45 °C depending on plasma treatment parameters.

2.2. Biotests

As a model of bacterial contamination of the surface, spores of *Geobacillus Stearothermophilus* deposited on stainless-steel discs (Raven Biological Laboratories, Inc., declared spore's population of 2.5×10^6) were used in this study. After the plasma treatment, the samples were examined by a scanning electron microscope (FEI Nova 600I Nanolab) in order to evaluate the degree of spores' destruction caused by the plasma treatment.

As an example of biomolecular contamination of surfaces bovine serum albumin (BSA) and brain homogenate (BrH) were selected. Microspotting of BSA and BrH samples on silicon wafers was performed using a Scienion S3 sciFLEXARRAYER (Scienion AG, Germany) spotter equipped with an automated piezo driven non-contact dispensing and with a three-axis micro-positioning system. A glass nozzle with a diameter of 80 μm was applied to generate drops of the 10 μg ml^{-1} solutions of BSA protein (from Fluka) and BrH dispersed in 5mM TrisHCl pH 7.5. Standard diameter and height of BSA and BrH spots obtained by this method were, respectively, around 40 μm and 200 nm. Ordered arrays of typically eight spots were deposited on each silicon substrate wafer. An integrated horizontal CCD camera allowed controlling drop volumes for determining the deposited protein amounts. BrH stock was prepared according to the method described in Viganò *et al* [29] and stored at −20 °C. Aliquots from the stock were thawed and used for suspensions preparation right before the microspotting.

Ellipsometry was used for *ex situ* non-contact optical characterization of protein layers [30]. For the acquisition of 2D maps of the ellipsometric Δ and Ψ angles, we employed a variable angle, multi-wavelength imaging ellipsometer (EP3, Nanofilm Surface Analysis GmbH). All measurements were performed in air at room temperature at an angle of incidence of 42° and a field of view of $2000\,\mu\text{m} \times 2000\,\mu\text{m}$. A monochromatized Xe-arc lamp was used as light source at 554.3 nm wavelength. A PCSA (polarizer–compensator–sample–analyser) null-ellipsometric procedure is used to obtain 2D maps of the Δ and Ψ angles [31]. The volume of protein droplets were determined from the ellipsometric parameters maps using standard classical electromagnetic theory in conjunction with a parallel layer model consisting of a silicon/silicon oxide/protein. The analysis of Δ and Ψ maps assumes that the total sample consists of semi-infinite parallel slabs, each a uniform material of homogeneous composition described by a single set of optical constants. The film thickness was determined using values for the substrate and film optical functions obtained by best fit of a set of three different incidence angle measurements.

Protein film mass removal was monitored *in situ* by a quartz crystal microbalance (QCM, Inficon) using the procedure described in our previous work [32]. The exposed area of the QCM crystal was $78.5\,\text{mm}^2$ and the BSA contamination level was $2.63 \pm 0.22\,\mu\text{g}\,\text{mm}^{-2}$. All QCM experiments were performed at a substrate temperature of $30 \pm 7\,^\circ\text{C}$ pulsing the plasma discharge and with water-cooling of the QCM crystal. The QCM crystal signal was monitored on line with a USB oscilloscope (Picoscope), by means of the external output voltage signal, proportional to the crystal frequency shift.

2.3. *Plasma characterization*

The relative ground state atom density in the plasma was estimated by optical emission actinometry. Photon emission from the plasma discharge was characterized by means of an Avantes AVS-PC2000 monochromator equipped with a 2048-element linear CCD array. Argon $2p_1 \rightarrow 1s_2$ transition at 750.4 nm, a common choice for actinometry [33], was not used because total argon flow was changed during most of the experiments, the Kr line at 826.3 nm ($E_{\text{th}} = 12.2$ eV) emission intensity from the Paschen $2p_2$ level was used to normalize emission intensities of O at 844 nm, H at 656 nm and OH at 309 nm. The dominant mechanism for excitation of the Kr $2p_2$ level is a one-step electronic excitation from the ground state and, in addition its energy threshold for this process is ($\sim$12 eV), near the respective excitations of O ($\sim$11 eV), H ($\sim$12 eV) and OH A–X ($\sim$10 eV). The actinometer used was introduced via dedicated line from a Kr bottle and its flow was kept under 5% of the total gas flow for all the experiments. Adding to the selected working gas mixture a small amount of Krypton in the range from 2% to 5% has been proven not to influence emission lines intensities of principal mixture components.

To measure the plasma parameters, a movable RF compensated Langmuir probe (SmartProbe®, Scientific Systems LTD) was used. Data acquisition was performed at the centre of the discharge chamber and at a vertical distance of 55 mm from the quartz glass facing the inductive antenna. This is the same position of the samples inserted in the reactor via the QCM diagnostic flange. Because of the presence of negative ions, the analysis of I/V characteristics was performed with a MatLab™ routine in the framework of the radial motion theory (thin sheath case), modified by the presence of negative ions [34].

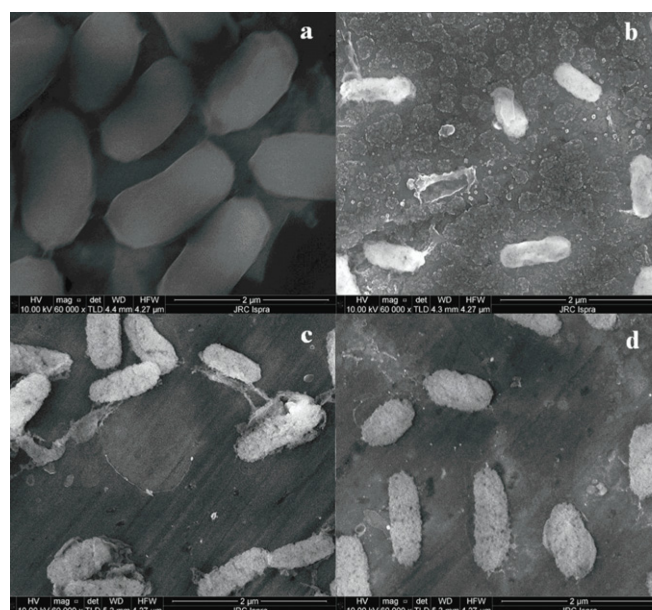

Figure 1. SEM images of (a) untreated and (b) H_2O, (c) O_2 and (d) H_2 plasma-treated spores (treatment time 5 min, power 500 W, pressure 10 Pa).

3. Results and discussion

The experimental results presented are divided into three sections. First, the efficacy of a water vapour discharge on bacterial spores (*Geobacillus Stearothermophilus*) as well as on BSA and BrH biomolecular contamination models is demonstrated and compared with other gas-phase plasma chemistries; second, the water vapour discharge particle fluxes are characterized by means of Langmuir and OES measurements and finally some mass removal experiments results are discussed in terms of the chemical sputtering removal mechanism.

3.1. *Water vapour plasma decontamination efficiency*

3.1.1. Bacterial Spores. Water vapour plasma efficacy for microorganism sterilization has been tested using stacked bacterial spore colonies deposited on stainless-steel discs. Figures 1(a)–(d) present SEM images of (a) untreated stacked spore colonies and spores exposed to (b) H_2O plasma discharge, as well as (c) O_2, and (d) H_2, plasma for comparison. Both control gas mixtures have been reported to be effective against bacterial spores when samples are exposed to the active region of the discharge [13, 35, 36] or to combined radicals

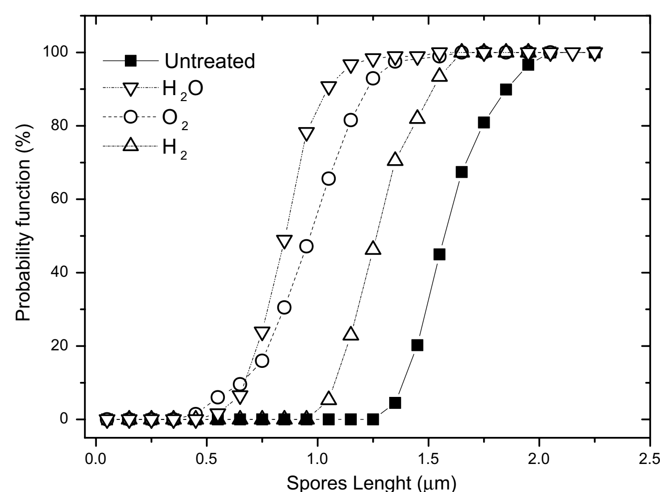

Figure 2. Spore sizes counts probability functions before (fill) and after (hollow) water vapour, oxygen and hydrogen plasma treatments. Common parameters are power 500 W, pressure 10 Pa and gas flow 10 sccm.

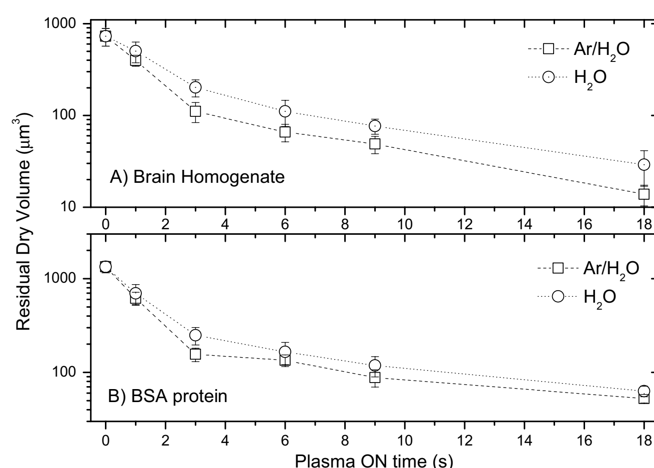

Figure 3. Residual dry volume measured by imaging ellipsometry of microspotted BrH (upper panel) and BSA protein (lower panel) after H_2O and Ar/H_2O [1 : 1] plasma discharge treatment. Plasma parameters are power 350 W, pressure 10 Pa and gas flow 10 sccm.

ion beams [27]. Only the gas composition was varied during experiments while all other process parameters (power 500 W, pressure 10 Pa and gas flow 10 sccm) were kept constant. As can be seen by comparison of figures 1(*b*), (*c*) and (*d*), after plasma exposition (pulsed plasma treatment, 100 mHz, 20% dc, t_{eff} = 5 min, $T_{substrate}$ < 45 °C) bacterial spores show similar morphological modifications on the outer surface and significant spores' sizes reduction.

Images' analysis on a statistically relevant number of spores (about 200 per each treated sample) were used to derive the probability distribution of spores' sizes before and after plasma treatment. Single spore shape with respect to background is approximated by an ellipse; the major axis length is considered an indicator for spores' sizes. Results summarized in figure 2 show that, under the specified treatment conditions, the spores' mean length is reduced from about 1.60 to 0.89 μm after 5 min. by water vapour plasma treatment. Similar experiments performed with oxygen and hydrogen plasma resulted in final spores' mean length of 1.02 μm and 1.29 μm, respectively, in agreement with our former results [37].

Longer treatment times experiments do not lead to further additional decrease in the spores' sizes and samples exposed for 10, 15 and 20 min to H_2O plasma show size distributions close to one reported in figure 2. Such a phenomenon was already reported [38] for oxygen containing discharges, and it was attributed to the increasing density of non-volatile compounds (e.g., calcium, sodium, etc) on the spores' external surfaces, forming an etching-resistant layer; the same process was also recently investigated on protein films' model contaminations [32].

Data from figure 2 indicate that H_2O plasma can interact and damage bacterial spores, most likely via a chemical sputtering mechanism. This erosion mechanism was reported to be dominant in the plasma ionization region [39], but in our case, water vapour plasma may also benefit from the potential contribution of UV emission from OH molecular band at 309 nm (see figure 5 in section 3.2), which was not observed in optical emission spectra of control discharges. Spores' erosion levels for water vapour plasma are comparable, and even slightly higher, than the results obtained using oxygen plasma. Hydrogen plasma shows lower efficacy in terms of average size reduction and a substantial overlap with the untreated spore size distribution.

3.1.2. Biomolecules. To test the potential efficiency of water vapour plasma against biological residuals, both BSA and BrH model contamination have been treated. After the plasma treatment with H_2O and Ar/H_2O ICP discharge, pronounced modifications of both protein and BrH films have been observed in the ellipsometric height-maps indicating a substantial removal of the protein deposit as shown in figure 3.

The volume of the dry residual is reduced, in both cases, by more than one order of magnitude after 18 s of plasma treatment indicating substantial volatilization of the biological film induced by the plasma. The dynamics of the biological films removal shows a two-phase behaviour: mass loss is faster (i.e. higher etching rates are observed) in the first 3 s of treatment when the initial volume is reduced to about 10% of its initial value, while for longer treatment times material removal phase appears to be much slower. This behaviour for thin biological films can be interpreted as the transition from etching of the bulk biological material to a non-etchable residuals covered surface as explained in [32].

To assess the efficiency of water vapour plasma decontamination in comparison with other gas-phase chemistries, BSA protein film mass loss induced by different discharge mixtures have been compared by means of *in situ* QCM measurements [32] (see figure 4). In these experiments, all the treatment parameters such as plasma-ON time, RF delivered power, gas pressure and gas flow were kept constant and for all the binary mixtures investigated the ratio of gas flows was 1 : 1, except for H_2/O_2 discharge the ratio used was 2 : 1, i.e. ratio of hydrogen to oxygen in water molecule. The substrate temperature was kept below 40 °C for all the experiments by

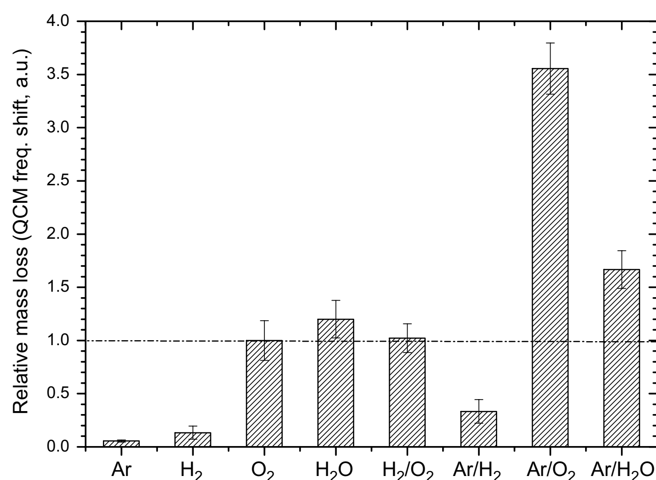

Figure 4. *In situ* QCM measurement of relative mass loss rates induced by different gas mixtures . BSA protein thin films are deposited on QCM crystals, average mass areal density is $2.63 \pm 0.22\,\mu g\,mm^{-2}$, fixed plasma treatment parameters are power 350 W, pressure 10 Pa, gas flow 10 sccm and effective treatment time 2 s. All binary mixtures gas flows ratio is [1 : 1], except H_2/O_2 mixture, which is [2 : 1]. Data are normalized to O_2 discharge mass loss rate.

pulsing the discharge and water-cooling the QCM case. Data have been normalized to pure oxygen discharge induced mass loss. As can be seen, discharges sustained in pure Ar and H_2 show little effect on the biological film while discharge in pure oxygen leads to significant removal. Both pure water vapour and 'synthetic' water vapour (H_2/O_2, 2 : 1) discharges show removal rates slightly higher than pure oxygen plasma (+20% for H_2O and +2% for H_2/O_2). These results are in agreement with the results obtained in experiments with bacterial spores.

In analogy with oxygen containing mixtures optimization strategies described in [9], an attempt was made to promote ion production by argon gas addition. Ar/H_2 discharge removal efficacy increases with respect to pure H_2, but the absolute rate remains negligible compared with oxygen or water vapour discharge. Ar/H_2O discharge shows a mass removal rate enhancement of 38% as compared with pure water vapour and of +66% as compared with pure oxygen, while being about two times less efficient than the Ar/O_2 mixture. Poor performances of the H_2 and Ar/H_2 discharges suggest that H atoms have little efficiency in the surface chemistry, while comparable removal rates between O_2, H_2O and H_2/O_2 discharges may indicate that oxygen radicals are crucial for fast volatilization of biological matters. These hypotheses will be investigated more carefully in the subsequent discussion.

From an applicative point of view, these data show that both pure water vapour plasma as well as Ar/H_2O plasma represent efficient alternatives for protein removal treatments.

3.2. Water vapour and Argon/water vapour plasma characterization

Figure 5 shows a typical optical emission spectrum of the inductively coupled water vapour plasma and in plasma sustained in 1 : 1 mixture of Ar and water vapour. Spectral signatures of O, H and OH radicals were observed in both

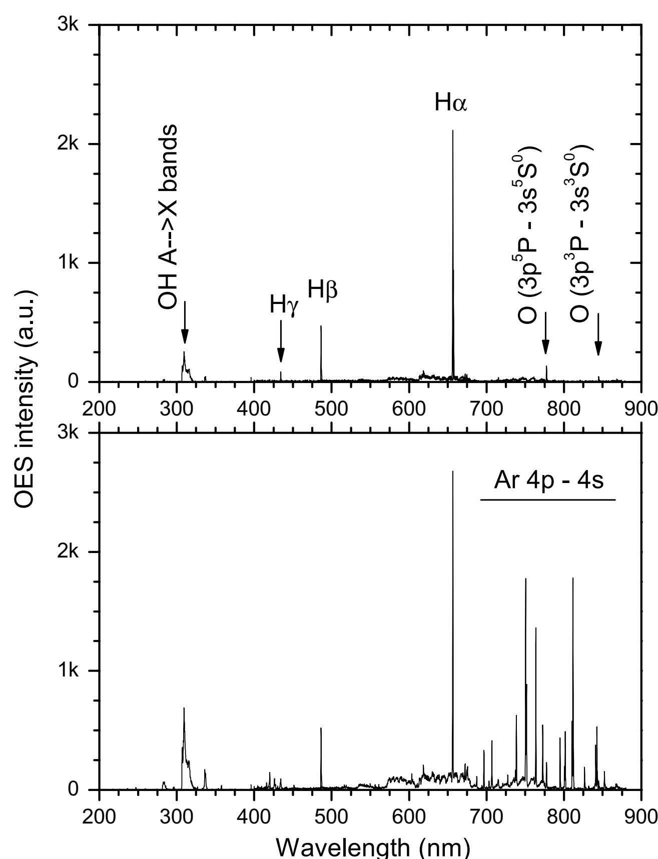

Figure 5. Upper panel: typical optical emission spectrum from a water vapour discharge. Lower panel: typical optical emission spectrum from Ar/H_2O [1 : 1] discharge. Plasma conditions are power 350 W, pressure 10 Pa and gas flow 10 sccm.

cases, while the respective peaks' intensities are in general higher in the Ar/H_2O discharge.

The characteristic low-pressure atomic lines of hydrogen (H_α at 656 nm, H_β at 486 nm and H_γ at 434 nm) and oxygen ($3p^5P$-$3s^5S$ at 777 nm and $3p^3P$-$3s^5S$ at 844 nm) were the most prominent. The (0,0) $A \rightarrow X$ transition of the OH molecular band at 309 nm was observed as well. As low intensity background between 600 and 775 nm molecular nitrogen vibrational bands, due to impurities present into the vacuum chamber, can be seen at larger integration times. All the radicals detected in the optical spectra have potential reactivity with organic materials, O and H atoms together with OH molecules can be produced through different electron impact water molecule dissociation processes [40].

An important parameter characterizing ICP discharge is transition between its E- and H-modes. E- to H-mode transition for a given gas mixture in ICP plasma depends on power and pressure and can be monitored by optical emission lines intensity, which rises with increasing power and suddenly changes to much higher values (up to 2 orders of magnitude) when the discharge turns into H-mode. The modes transition was identified by monitoring the intensity of the H atomic line at 656 nm as a function of the delivered RF power.

Transition power is observed to shift towards higher values when the pressure increases, meaning that sustainment of the inductive mode requires more power due to the decreased

Table 1. RF delivered power required for E to H-mode transition for Ar, H_2O and Ar/H_2O (1 : 1) discharges, total gas flow was kept constant at 22 sccm.

	E to H transition power density (mW cm^{-3})		
Pressure (Pa)	Ar	Ar/H_2O	H_2O
2.5	6 ± 1	19 ± 1	26 ± 2
5.0	7 ± 1	23 ± 2	30 ± 2
10.0	8 ± 1	38 ± 2	44 ± 2
20.0	13 ± 1	44 ± 2	54 ± 2

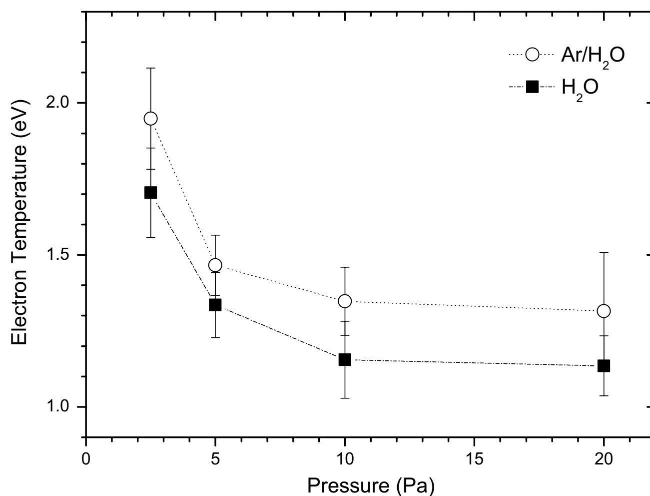

Figure 6. Electron temperature derived from Langmuir characteristics as function of operating pressure Argon/H_2O and H_2O discharge. Fixed plasma parameters are Ar/H_2O [1 : 1], total gas flow 10 sccm and power density 0.08 W cm^{-3}.

mean free path experienced from the capacitively generated electrons. As soon as water vapour is introduced in the gas mixture, the power required for mode transition increases abruptly (see table 1). This is explained by considering the energy supplied by the electrons in order to sustain the gas-phase chemistry of the water molecules, which is not available anymore to sustain ionization processes. In some cases, e.g. electron attachment process, the water molecule plasma chemistry acts as an electron sink thus pushing the transition threshold to higher energies. As long as the water vapour fraction in the mixture is increased, the importance of loss processes increases, determining higher transition powers required for the mode transition.

Hereafter (figures 6 and 7) positive ion density and electron temperature are derived from measured Langmuir characteristics recorded at the centre of the discharge. As is common for this class of discharges, the electron temperature in ICP is mainly controlled by ionization balance [41] resulting in an inverse dependence from the working gas pressure and a typical length size for the plasma and practically does not depend on plasma density and discharge power. Indeed, it is found that also in our discharge, electron temperature decreases with increasing pressure, as shown in figure 6.

Particles number density (figure 7) derived from Langmuir characteristics is decreasing with increasing pressure and is found to be linearly dependent on discharge power in the

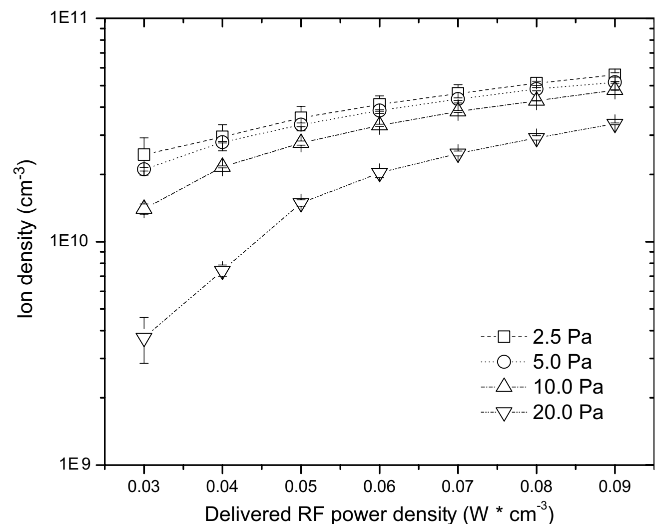

Figure 7. Positive ion density derived from Langmuir characteristics as function of operating pressure for several RF delivered power density values. Fixed plasma parameters are Ar/H_2O [1 : 1] and gas flow 10 sccm. Values in the circle correspond to E mode of the discharge.

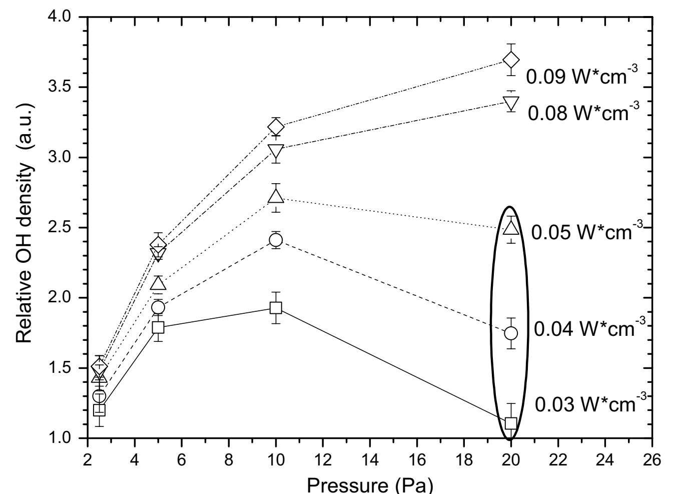

Figure 8. OH molecule density as a function of the discharge pressure for several RF delivered power density values. Plasma parameters are Ar/H_2O [1 : 1] and gas flow 10 sccm. Values in the circle correspond to E mode of the discharge.

inductive H-mode region. Data points corresponding to measurements on Ar/H_2O discharge at 20 Pa with less than 0.05 W cm^{-3} of RF delivered power show deviations from the linear trend. Nevertheless, it has to be noted that in this parameter region, we observe that the discharge ignites in the E mode.

Figure 8 shows the intensity ratio between 309 nm OH band head and the 826 nm Kr line, chosen as actinometer, as a function of the pressure in an Ar/H_2O discharge. All intensities are corrected for the instrument spectral calibration curve. Parametric dependence from RF delivered power density is plotted. The line intensity ratio is proportional, under actinometric assumptions, to the OH molecular radical density in the plasma. For Ar/H_2O discharge parameters combinations allowing plasma ignition directly in the H-mode

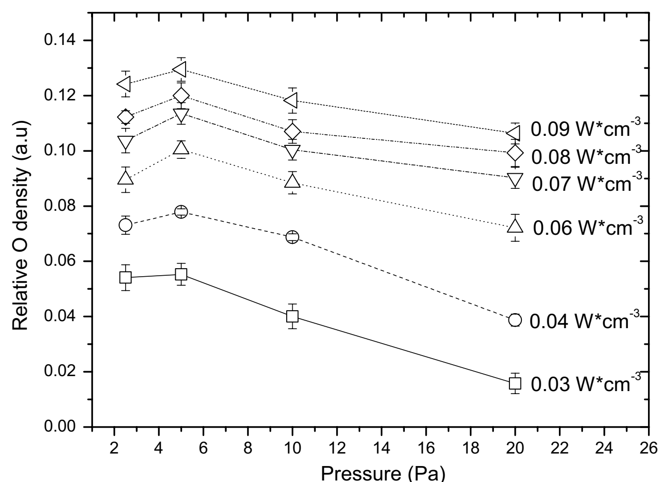

Figure 9. O atom density as a function of the discharge pressure for several RF delivered power values. Plasma parameters are Ar/H_2O [1 : 1] and gas flow 10 sccm.

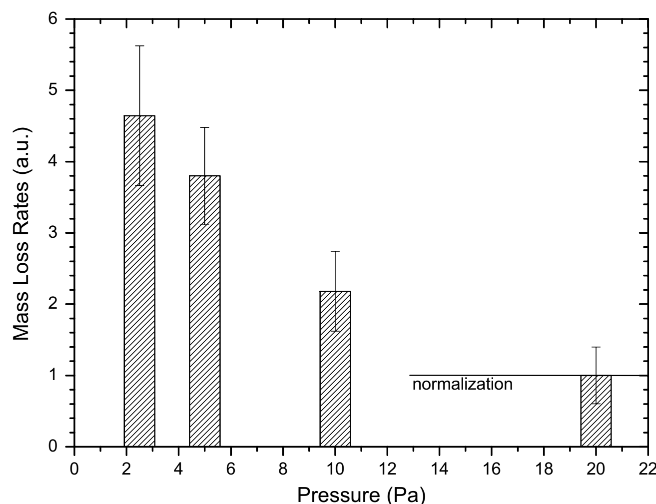

Figure 10. *In situ* QCM measurement of water vapour plasma induced relative mass loss rates. BSA covered QCM crystals, fixed plasma parameters are Ar : H_2O = [1 : 1], power 400 W, pressure 10 Pa, gas flow 10 sccm and treatment time 60 s. Data are normalized to the 20 Pa discharge mass loss rate.

the concentration of OH molecules increases when either pressure or power is increased in the investigated range.

Hydroxyl radical concentrations corresponding to 0.03, 0.04 and 0.05 W cm^{-3} in the discharge ignited at 20 Pa (points in the black circle in figure 6) are lower than the corresponding power levels at 10 Pa, for these three data points OH density shows a peak value at 10 Pa. This different behaviour is attributed to the fact that in this parameter region, the discharge is ignited in the E mode and the density of electrons available for impact dissociation reaction decreases.

Figure 9 shows the intensity ratio between the 844 nm O atom line and the 826 nm Kr line, chosen as actinometer, as a function of the pressure in an Ar/H_2O discharge. All intensities are corrected for instrument spectral calibration curve. Parametric dependence from RF delivered power is plotted. The line intensity ratio is proportional, under actinometric assumptions, to the O atomic radical density in the plasma. In the pressure range investigated, the concentration of O atoms initially increases with pressure and then shows a peak value at 5 Pa. For higher operating pressures, all the densities decrease when increasing the pressure.

The peak is explained by two competitive effects: first, the H_2O molecule density increases with increasing pressure (as a reactant for the production of O in the reaction $e + H_2O \rightarrow O*(3s^3S^0) + H_2(X) + e$ [40] or second order electron impact dissociation reactions of OH molecule), so one would expect a monotonic increase in the emission intensity as the pressure is increased. Second, however, both the electron temperature and electron density decreases with increasing pressure. Since the emission occurs in transitions from the excited states close to 11 eV, this factor becomes dominant at higher pressure. The delivered RF power density dependence shows that O atoms' concentration increases with delivered power (proportional to the electron density) in all the parameter range investigated.

3.3. Role of the radicals

Mass loss rates for BSA protein were derived by QCM measurements data for the first 60 s of plasma treatments. Every etching rate value is the average of five independent measurements. Column bars in figure 10 show the measured pressure dependence of the mass loss rates and corresponding errors at fixed power density and discharge mixture composition (0.09 W cm^{-3} and Ar : H_2O [1 : 1]). For better comparison, all the data are normalized to the mass loss rate measured at 20 Pa. It can be seen that as the pressure is increased, the efficacy of the plasma removal drops significantly: mass removal is more than four times slower at 20 Pa as compared with the etching rate measured at 2 Pa.

The dependence of the measured mass loss rates shown in figure 8 is explained according to the process of chemical sputtering [39], postulating that the combined interaction of ions and chemically reactive species with the surface is important for an efficient removal of biomolecules. Chemical sputtering was already proven to be a solid framework for sterilization and biomolecules etching data interpretation [27, 42–44]. Plasma characterization described in the previous section provides a dataset for reactive particle fluxes, which are proportional to the bulk densities of radical atoms and molecules as measured by actinometry. The ion flux is a function of the ions bulk density and the electron temperature as measured by Langmuir probe experiments.

As a rough hypothesis, it is possible to state that the mass loss rate is proportional to the product of ion flux and oxygen species flux, as already illustrated [45] for plasma etching of a hydrogenated carbon film. The model equation has the form

$$\mathrm{ER} = \mathrm{const} \cdot \Gamma_{\mathrm{ion}} \cdot \Gamma_{\mathrm{radical}}, \quad (1)$$

where ER is the mass removal rate, const is a proportionality constant and Γ_{ion} and $\Gamma_{radical}$ are the ion and radical fluxes directed to the surface.

The possibility of a leading role of hydrogen atoms in the surface chemistry is ruled out by results of the experiments shown in figure 4, where hydrogen containing mixtures show

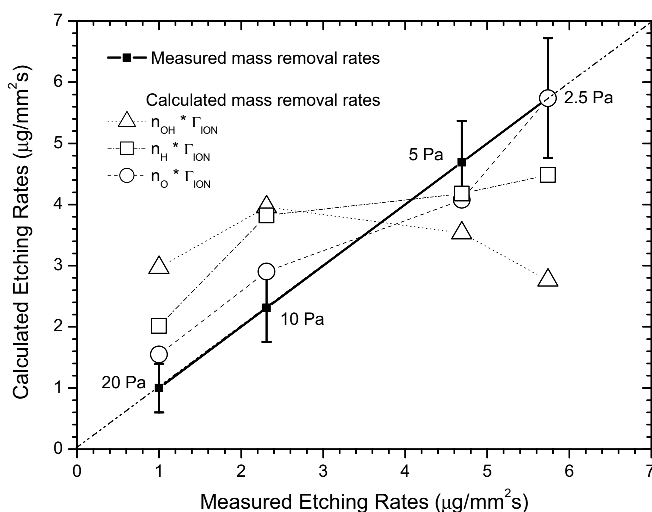

Figure 11. Measured BSA protein mass removal rates in Ar/H_2O discharge at different pressures (see figure 10) plotted against etching rates calculated using equation (1) and different radicals densities. Solid black line shows the measured mass removal rates values.

little effect on the biomolecules film, at a level comparable to non-reactive argon discharges. The hypothesis of the chemical sputtering process chemically driven by oxygen atoms adsorption on the protein surface is tested by plotting the product of ion flux and O densities ($n_O \times \Gamma_{ion}$) dependence of the working pressure of the discharge. In figure 11, another model ($n_{OH} \times \Gamma_{ion}$) is tested as well; in this case it is assumed that the adsorbed hydroxyl radicals react on the surface to form a chemical compound that can be removed by ion bombardment, leading to biomaterial removal.

The overall behaviour of the measured mass loss rate (ER_m) is well reproduced by the mass removal rates calculated using the best parameter estimate obtained regressing the particle fluxes dataset using an equation of the form $ER_m =$ const $\times\, n_O \times \Gamma_{ion}$, while the values calculated using OH molecules and H atoms densities and the same equation structure cannot reproduce the trend of the measured mass loss rates. For pure hydroxyl and hydrogen chemistries the calculated datasets are heavily skewed with respect to the real measurements.

This result indicates that oxygen radicals play a major role in water vapour plasma chemical sputtering of protein films. However, even if the mass loss values calculated using the oxygen atom density reproduce the parametric discharge pressure dependence, the magnitude of the model residuals are comparable to the magnitude of the experimental error on the mass removal rates. The possibility of secondary mechanisms involving contribution of hydroxyl molecule to the overall process cannot be absolutely ruled out.

Two possible contributions to the removal mechanism can be associated with the OH molecule itself. First emission of the excited molecular state OH A–X at 309 nm in the UV region may promote protein removal rates by photodissociation processes on the surface [46]. Second, hydrogen abstraction processes by OH radicals has been reported [47] as being an effective reaction in surface chemistry of water vapour plasma–protein films interaction. Rate constants for H-abstraction processes from hydrocarbons by OH radicals are 3 orders of magnitude faster than the hydrogen atom driven H-abstraction and two orders of magnitude faster than oxygen atom driven H-abstraction reactions [48]. Even if the initial H-abstraction event is not a direct fragmentation reaction that attacks the protein structure, the resulting radical centre formed on the biomolecule may produce in a surface site that is activated for chain scission reactions driven by oxygen atoms, thus contributing to enhance mass removal rates above the values calculated using only pure oxygen chemistry.

4. Conclusions

While the use of oxygen-based plasma discharges for biomolecules decontamination has been studied in detail in the past few years, relatively fewer results have been published concerning the removal of proteins and biological matrices from surgical instruments by means of a water vapour discharge. Recent studies [49, 50] revealed, however, that the present decontamination medical protocols show little efficacy. Therefore, the possibility to eliminate biomolecular contaminations by low-pressure H_2O plasma treatment was addressed in this study.

Plasma decontamination of silicon surfaces or stainless-steel discs was achieved using water vapour plasma; model contaminations created either with colonies of bacterial spores, pure protein films or with biological matrices were effectively reduced by the interaction with the H_2O plasma on a reasonable time scale. Mass removal rates for water-vapour-based discharges and the general efficacy of such plasmas are found to be comparable to oxygen-based discharges operated under identical conditions. This result indicates that a water-vapour-based mixture might be used to implement an efficient cost-effective decontamination device.

Water vapour plasma discharges were characterized by means of optical emission spectroscopy and Langmuir probe, and plasma fluxes were measured under several operating parameters' conditions ranging from 2 to 20 Pa and 0.03 to 0.09 W cm^{-3}. Plasma fluxes data have been used to predict mass removal rates behaviour within the framework of chemical sputtering plasma biomaterial interaction mechanism. Comparison of different interaction schemes indicates that the leading interaction is chemically favoured by oxygen atoms' reactions on the surface. Oxygen atoms' contribution to mass removal rates cannot alone fully explain the measured data, it is postulated that hydroxyl molecules play an auxiliary role both in terms of UV emission and H-abstraction processes.

Acknowledgments

This work is based upon work supported by the Nanobiosciences project at the JRC, Institute for Health and Consumer Protection. We thank Dott. Fabio Franchini for helpful discussions.

References

[1] Lipscomb I P, Sihota A K and Keevil C W 2006 *J. Clin. Microbiol.* **44** 3728
[2] Murdoch H, Taylor D, Dickinson J, Walker J T, Perrett D, Raven N D H and Sutton J M 2006 *J. Hospital Infection* **63** 432
[3] Taylor D M 1999 *J. Hospital Infection* **43** S69
[4] Lerouge S, Guignot C, Tabrizian M, Ferrier D, Yagoubi N and Yahia L H 2000 *J. Biomed. Mater. Res.* **52** 774
[5] Nair P D 1995 *J. Biomater. Appl.* **10** 121
[6] Mazzu A L and Smith C P 1984 *J. Biomed. Mater. Res.* **18** 961
[7] Ryan K J, Ray C G, Champoux J J, Neidhardt F C, Drew W L and Plorde J J 2004 *Sherris Medical Microbiology: an Introduction to Infectious Diseases* ed K J Ryan, C G Ray and J C Sherris (New York: McGraw-Hill) pp 175–85
[8] Prusiner S B 1998 *Proc. Natl Acad. Sci.* **95** 13363
[9] Kylián O and Rossi F 2009 *J. Phys. D: Appl. Phys.* **42** 085207
[10] Kylián O, Rauscher H, Gilliland D, Bretagnol F and Rossi F 2008 *J. Phys. D: Appl. Phys.* **41** 095201
[11] Rauscher H, Stapelmann K, Kylián O, Denis B and Rossi F 2009 *Vacuum* **84** 75
[12] Baxter H C, Campbell G A, Richardson P R, Jones A C, Whittle I R, Casey M, Whittaker A G and Baxter R L 2006 *IEEE Trans. Plasma Sci.* **34** 1337
[13] Rossi F, Kylián O and Hasiwa M 2006 *Plasma Process. Polym.* **3** 431
[14] Rossi F, Kylián O and Hasiwa M 2008 *Advanced Plasma Technology: Mechanisms of sterilization and decontamination of surfaces by low-pressure plasma* ed R d'Agostino, P Favia, Y Kawai, H Ikegami, N Sato and F Arefi-Khonsari (Wiley-VCH Verlag GmbH & Co. KGaA) p 319–40
[15] Philip N, Saoudi B, Crevier M C, Moisan M, Barbeau J and Pelletier J 2002 *IEEE Trans. Plasma Sci.* **30** 1429
[16] Boudam M K, Saoudi B, Moisan M and Ricard A 2007 *J. Phys. D: Appl. Phys.* **40** 1694
[17] Boudam M K and Moisan M 2010 *J. Phys. D: Appl. Phys.* **43** 295202
[18] Vujošević D, Mozetič M, Cvelbar U, Krstulović N and Milošević S 2007 *J. Appl. Phys.* **101** 103305
[19] Cvelbar U, Vujošević D, Vratnica Z and Mozetič M 2006 *J. Phys. D: Appl. Phys.* **39** 3487
[20] Suzuki T, Saburi T, Tokunami R, Murata H and Fujii Y 2006 *Thin Solid Films* **506–507** 342
[21] Steen M L, Hymas L, Havey E D, Capps N E, Castner D G and Fisher E R 2001 *J. Membr. Sci.* **188** 97
[22] Steen M L, Jordan A C and Fisher E R 2002 *J. Membr. Sci.* **204** 341
[23] Weikart C M and Yasuda H K 2000 *J. Polym. Sci.* A **38** 3028
[24] Oh J S, Kawamura K, Pramanik B K and Hatta A 2009 *IEEE Trans. Plasma Sci.* **37** 107
[25] Hayashi N, Tsutsui S, Tomari T and Guan W 2008 *IEEE Trans. Plasma Sci.* **36** 1302–3
[26] Kregar Z, Krstulović N, Vukelić N G and Milošević S 2009 *J. Phys. D: Appl. Phys.* **42** 145201
[27] von Keudell A *et al* 2010 *Plasma Process. Polym.* **7** 327
[28] Kylián O, Rauscher H, Denis B, Ceriotti L and Rossi F 2009 *Plasma Process. Polym.* **6** 848
[29] Viganò D, Rubino T, Vaccani A, Bianchessi S, Marmorato P, Castiglioni C and Parolaro D 2005 *Psychopharmacology* **182** 527
[30] Arwin H 2000 *Thin Solid Films* **377–378** 48
[31] Tompkins H G and Irene E A 2005 *Handbook of Ellipsometry* (Heidelberg: Springer) p 12
[32] Fumagalli F, Hanuš J, Kylián O and Rossi F 2011 *Plasma Process. Polym.* (Early view online DOI: 10.1002/ppap.201100098)
[33] Czerwiec T, Greer F and Graves D B 2005 *J. Phys. D: Appl. Phys.* **38** 4278
[34] Riccardi C, Barni R and Fontanesi M 2001 *J. Appl. Phys.* **90** 3735
[35] Kylián O, Sasaki T and Rossi F 2006 *Eur. Phys. J.—Appl. Phys.* **34** 139
[36] Halfmann H 2007 *J. Phys. D: Appl. Phys.* **40** 4145
[37] Rossi F, Kylián O, Rauscher H, Hasiwa M and Gilliland D 2009 *New J. Phys.* **11** 115017
[38] Lerouge S, Wertheimer M R, Marchand R, Tabrizian M and Yahia L H 2000 *J. Biomed. Mater. Res.* **51** 128
[39] Rauscher H, Kylián O, Benedikt J, von Keudell A and Rossi F 2010 *ChemPhysChem* **11** 1382
[40] Itikawa Y and Mason N 2005 *J. Phys. Chem. Ref. Data* **34** 1
[41] Gudmundsson J T 2001 *Plasma Sources Sci. Technol.* **10** 76
[42] Kylián O, Benedikt J, Sirghi L, Reuter R, Rauscher H, von Keudell A and Rossi F 2009 *Plasma Process. Polym.* **6** 255
[43] Opretzka J, Benedikt J, Awakowicz P, Wunderlich J and Keudell A v 2007 *J. Phys. D: Appl. Phys.* **40** 2826
[44] Raballand V, Benedikt J, Wunderlich J, and Keudell A v 2008 *J. Phys. D: Appl. Phys.* **41** 115207
[45] Benedikt J, Flotgen C, Kussel G, Raball V and von Keudell A 2008 *J. Phys.: Conf. Ser.* **133** 012012
[46] Stapelmann K, Kylián O, Denis B and Rossi F 2008 *J. Phys. D: Appl. Phys.* **41** 192005
[47] Stalder K R, McMillen D F and Woloszko J 2005 *J. Phys. D: Appl. Phys.* **38** 1728
[48] Baulch D L *et al* 1992 *J. Phys. Chem. Ref. Data* **21** 411
[49] Herve R, Secker T J and Keevil C W 2010 *J. Hospital Infection* **75** 309
[50] Lipscomb I P, Herve R, Harris K, Pinchin H, Collin R and Keevil C W 2007 *J. Gen. Virol.* **88** 2619–26